

UDK 666.982.7; 622.785

## **Anisotropy Analysis of Low Cement Concrete by Ultrasonic Measurements and Image Analysis**

**Sanja P. Martinović<sup>1</sup>, Milica M. Vlahović<sup>1\*)</sup>, Jelena B. Majstorović<sup>2</sup>,  
Tatjana D. Volkov Husović<sup>3</sup>**

<sup>1</sup>University of Belgrade, Institute of Chemistry, Technology and Metallurgy, Dept. of Electrochemistry, Njegoseva St., 4 Karnegijeva St., Belgrade, Serbia

<sup>2</sup>University of Belgrade, Faculty of Mining and Geology, 7 Djusina St., Belgrade, Serbia

<sup>3</sup>University of Belgrade, Faculty of Technology and Metallurgy, 4 Karnegijeva St., Belgrade, Serbia

---

### **Abstract:**

*The analyzed material was high alumina low cement castable sintered at three different temperatures. Influence of initial material anisotropy on the thermal shock resistance as well as changes of anisotropy level during the thermal shock were studied. Water quench test was used as an experimental method for the thermal stability testing. Surface anisotropy was analysed by image analysis and structural anisotropy using ultrasonic measurements. The results pointed out that the highest homogeneity and the lowest surface and structural anisotropy was for the samples sintered at 1600 °C. Surface anisotropy had prevailing influence on behavior of material during the thermal shock, but the structural anisotropy should not be neglected.*

**Keywords:** Refractories; Anisotropy; Image analysis; Ultrasonic measurements; Low cement concrete

---

## **1. Introduction**

Refractory castables, also known as refractory concretes, are the most important group of monolithic refractories. Today's dense low and ultra-low cement refractory castables are very complex composition of aggregate, cement, water, fine and ultrafine fillers, additives, and deflocculants designed in accordance with packing model that provides optimal packing of particles [1,2]. Refractory concrete should be considered as two-phase composite, consisted of a matrix surrounding a skeleton of coarse aggregate grains. Based on the literature [3-9], all fractions of castable components finer than 45 µm make a matrix. Coarser particles ( $\geq 45$  µm) that make an aggregate are considered as an inert component, since they do not participate in formation of hydratable phases. Properties of the concretes are strongly dependant on phase composition, microstructure, and reactions between constituents inside the matrix [10,11]. Actually, many properties of materials depend strongly on the structure, even if the composition of material remains the same. Generally, the properties of refractory concrete depend on characteristics of raw materials and processing procedure or synthesis. Also, the treatment after synthesis that include curing, drying, and

---

\*) **Corresponding author:** milica.vlahovic@yahoo.com

sintering play very important role, since they have influence on formation of final microstructure (creation of typical phases, discontinuities, porosities, vacancies, and cracks). All refractory materials and therefore concretes contain numerous of errors or defects in the form of flaws, pores, microcracks, and impurities in the structure. The presence of defects in the structure is considered as undesirable because they can deteriorate the properties of material, such as strength, wear, corrosion, abrasion, elasticity, and thermal shock resistance. Defects or flaws occur randomly throughout the structure inducing the variations in values of measured properties [12,13]. Quantification of direction-dependent variables such as level of defects could be an important tool to predict changes of some properties. For the first time, an ultrasonic technique in combination with the surface image analysis were applied to access anisotropy analysis of referent casting vibro-concrete as well as to monitor the anisotropy changes during thermal shock. Both applied techniques can be classified as non-destructive (NDT), a specific procedure whereby samples are not changed throughout the test in any way and can be reused again.

Ultrasonic measurements provide important information about the mechanical, anisotropic, and elastic properties of medium through it passes. Usually, the ultrasonic measurements are used for determination of materials (a) elasticity, (b) microstructure (grain size, texture, density), (c) discontinuity (porosity and damages), and (d) mechanical properties (tensile strength, shear strength, hardness etc.). Ultrasonic measurement techniques are widely used for the characterization of ceramic, refractory, and building materials [14-23]. Mechanical properties at different directions and temperatures can be determined by measurement of ultrasonic velocity which is useful for analysis of material structure and its anisotropy. Traditional forming techniques for ceramic compacts such as extrusion, slip casting, tape casting and pressing often lead to textured materials due to anisotropically shaped particles [14,24]. Materials behavior can be predicted and simplified by a precise knowledge of the direction-dependent microstructure. This approach is well established in the field of geophysics, where the evaluation of anisotropy in rocks is fundamental and is generally investigated by ultrasonic measurements. Morphology of casting refractory concrete form oriented phases and defects under the influence of gravity thus induce anisotropy. In this study, the longitudinal ultrasonic wave velocity was monitored and measured parallel to the direction of casting.

Materials surface anisotropy is quantified as degradation level per sides of samples. Image analysis was used for determination of level degradation that is adopted as a level of materials open porosity. The pore structure depends on the synthesis conditions like compaction pressure, sintering temperature, and time. If the pores are similar in shape and distributed in homogeneous pattern then a good justification of mechanical property can be obtained. Anisotropic behavior of composites such as refractory concretes formed by the mixing of two or more materials is reflected in different mechanical properties depending on their composition.

In this paper, the influence of sintering temperature on low cement castable anisotropy and therefore their structure on thermal shock behavior will be discussed. Non-destructive testing methods, such as image analysis and ultrasonic measurements, are possible techniques for obtaining deep insight of material anisotropy as they provide powerful methodology for monitoring the changes at the surface and inside the samples during the thermal stability testing.

## **2. Experimental**

### **2.1 Materials**

Initial components used for preparation refractory concrete, more precisely low cement castable, were commercially available raw materials: tabular alumina (T-60, Almatis)

used as an aggregate, fine and ultra fine fractions of tabular alumina, and reactive alumina as a filler (CL-370, Almatiss), calcium-aluminate cement (CA-270, Almatiss), and dispersing aluminas as an additive (ADS-3 and ADW-1, Almatiss). In order to obtain optimum particle packing, and therefore maximum density and sufficient porosity, particle size distribution was adjusted to the theoretical curve based on the Andreassen's packing model with the distribution coefficient  $q$  of 0.25, maximum grain size of 5 mm, and dry mixture density of  $3.75 \text{ g/cm}^3$ . Also, continuous particle size distribution was applied where all particle sizes were present: tabular and reactive alumina from 0 to 5 mm and calcium aluminates cement with  $d_{50}$  of  $6 \mu\text{m}$ . First, dry components were mixed for 2 minutes and then deflocculated containing water (water dispersed with citric acid) was added and mixing continued for another 4 minutes. Content of deflocculant was 4.67 wt. % (dry basis), and water/cement ratio was almost 1 ( $w/c \approx 1$ ). The obtained mixture was cast in steel moulds by vibration. The cubes of 4 cm edge length were prepared for further testing. After curing, the samples were sintered at 1100, 1300, and 1600 °C for 3 hours and cooled down to the room temperature inside the furnace. Prepared samples were subjected to the analysis of anisotropy as well as to the water quench test.

## 2.2 Methods

### 2.2.1 Image analysis

Level of surface degradation that actually presents level of defects per sides of samples were used for the analysis of materials surface anisotropy. Image analysis was realized by Image Pro Plus Program for the surface degradation study [25]. By this way, monitoring of surface defects level was possible by taking and analysing photographs of samples surface areas before and during the thermal shock [2,10,12,26-31]. Anisotropy of samples surface is based on determination of differences between damaged and undamaged areas. All results of degradation levels were calculated and compared to the ideal surface and they were presented in percentages  $(P/P_0) \cdot 100 \%$ . Since all ceramic and refractory materials have certain quantity of defects, pores, micropores, and cavities after the synthesis and treatment, certain level of surface degradation is expected before the tests.  $P_0$  is initial surface degradation that was determined according to the ideal facets area of  $4 \text{ cm} \times 4 \text{ cm}$  ( $16 \text{ cm}^2$ ).  $P$  presents measured damaged surface in  $\text{cm}^2$ . Five surfaces of each cubic sample were photographed and analyzed, while the sixth was used for marking. Analyzed surfaces were marked by different colors with the aim of obtaining better resolution and simplifying differentiation between damaged and undamaged areas. The damages of surface structure are presented as a portion of the damaged surface area.

### 2.2.2 Ultrasonic measurements

Morphology of casting refractory concrete is consisted of oriented phases and defects that are formed under the influence of gravity thus inducing anisotropy. Also, content of presented phases and defects depends on sintering temperature. The mechanical behaviour and anisotropic properties of the material can be well defined based on the knowledge of ultrasonic velocity. The low intensity and high frequency ultrasonic waves are applied for material characterization. The most common mode of propagation an ultrasonic wave in a medium utilize the longitudinal waves or transversal waves. Longitudinal and transversal wave velocities are more important for the material characterization because they are well related to elastic constants and density. The stress strain relationships for anisotropic crystals vary with the direction. Thus velocity of ultrasonic wave varies with the direction of propagation of wave and mode of polarization. There are three type of ultrasonic velocity (one longitudinal and

two shear waves) for each direction of propagation of wave in cubic and hexagonal structured materials [32-34]. In this study, the longitudinal ultrasonic wave velocity was measured parallel to the direction of casting.

The UPVT method has been considered in detail in Refs. [10,12,26,27,29,30]. Briefly, pulses of longitudinal elastic stress waves are generated by an electro-acoustical transducer that is held in direct contact with the surface of the sample under test. After traveling through the material, the pulses are received and converted into electrical energy by another transducer. Most standards describe three possible arrangements for the transducers:

- 1) the transducers are located directly opposite each other (direct transmission),
- 2) the transducers are located diagonally to each other; that is, the transducers are across corners (diagonal transmission),
- 3) the transducers are attached to the same surface and separated by a known distance (indirect transmission).

The velocity,  $V$ , is calculated from the distance between the two transducers and the electronically measured transit time of the pulse as:

$$V(m/s) = \frac{L}{T} \quad (1)$$

where  $L$  is the path length (m) and  $T$  is the transit time (s).

The measurement of ultrasonic velocity was performed using the equipment OYO model 5210 according to the standard testing procedure (ICS 81.080 SRPS D.B8.121.). The transducers were rigidly placed on two parallel faces of the cube shaped sample using vaseline grease as a coupling medium. The ultrasonic velocity was then calculated from the spacing of the transducers and the wave from time delay on the oscilloscope.

### 2.2.3 Water quench test

Since the refractory concretes are used usually in conditions of cyclic temperature changes, prepared samples were subjected to the test of thermal shock resistance. As an experimental method for investigation of the thermal shock behavior, water quench test was applied (ICS 81.080 SRPS B.D8.308). Each thermal shock cycle consisted of several consequent steps: slow heating up by a nominal heating speed of 10 °C/min to the quench temperature set at 950 °C, keeping the samples at this temperature for 30 minutes to reach thermal equilibrium throughout the specimen volume and finally the quenching into the water bath at temperature of 23 °C. This is the destructive test method which is similar to the procedure described in PRE Refractory Materials Recommendations 1978 (PRE/R5 Part 2).

## 3. Results and discussion

The idea was to analyze the influence of structural and surface anisotropy of refractory concrete with three different structures on the thermal shock resistance. Two non-destructive methods were applied: image analysis with the aim of observing surface anisotropy and ultrasonic measurements due to study of internal structure homogeneity. An attempt was made to examine whether the surface or internal anisotropy has more influence on behavior of material subjected to the thermal shock and how they have changed during the testing.

### 3.1 General characterization of analyzed samples

Beside the phase composition which is the result of reactions between the constituents of the matrix, structural and microstructural appearance of material has the strong influence

on many concrete properties and thus on thermal shock resistance. As it is already mentioned, all refractory concretes contain numerous of defects in the form of flaws, pores, microcracks, and impurities occurred randomly throughout the structure inducing the variations in properties. Therefore, focus of the study was the analysis consisting of quantification of direction-dependent structure such as level of defects, an important tool to predict variations of physical properties. Initially, investigated samples were subjected to the determination of apparent density and porosity. Reference or cured samples as well as the samples sintered at 1100, 1300, and 1600 °C, before exposure to the thermal shock, were tested. The apparent density was determined according to the immersion tests by standard laboratory procedure SRPS B.D8.302 using boiling water saturation technique. The true porosity was estimated based on the SEM micrograph and image analysis using of Image Pro Plus program. Results are shown in Fig. 1.



**Fig. 1.** Change of apparent density and true porosity vs. treated temperature.

Apparent density, as expected, was growing with increase of sintering temperature but almost negligible. The initial true porosity was generally quite low ( $< 5\%$ ), probably because of several reasons: small value of apparent porosity of coarse aggregate tabular alumina which was  $\leq 5\%$ , small amount of microcracks between large aggregates and matrix, and the formation of  $AH_3$ -stable gelatinous phase that can close pores between interfacial defects and form denser structure filled with the gel. Results showed that the true porosity was increasing with the temperature of materials' sintering.

Surface anisotropy was monitored by determining surface degradation levels that implies calculation of differences between the highest and the lowest degradation levels among five surface sample sides. On the other side, structural anisotropy was analyzed by measurements of ultrasonic velocities of longitudinal waves (parallel to the casting gravity direction) in three different directions. Results are given in Figs. 2 a) and b), respectively.

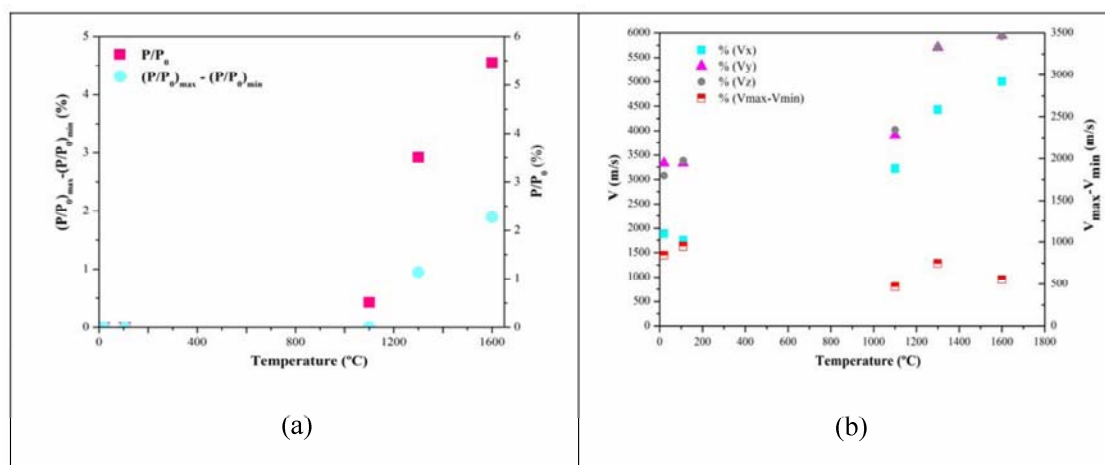


**Fig. 2.** Surface (a) and structural (b) degradation of initial samples.

Surface anisotropy analysis was based on determination of defects and pores quantities per surface sides of the cubic sample. As an indicator of surface anisotropy, dissipation-differences among the levels of degradation per surface sides were used. If the difference between maximum and minimum values is smaller, it can be assumed that observed material has higher homogeneity and smaller surface anisotropy. It is evident that different sides of the sample surfaces have different values of damage level indicating that the level of surface degradation is direction-dependent. Also, the difference between the highest and the lowest values of surface damage increase with increasing of sintering temperature, so that the samples sintered at 1100 °C has negligible anisotropy with isotropic, almost homogeneous surface structure, while the samples sintered at 1300 and 1600 °C show higher values of surface inhomogeneity and initial anisotropy.

As it was already mentioned, ultrasonic measurements were used for the analysis of structural homogeneity and anisotropy. Since the theory proves that ultrasonic pulse travels with lower velocity through the material of higher porosity and lower density, methods of measuring ultrasonic velocity can be used for monitoring the changes in the materials structure. Based on the ultrasonic measurements of longitudinal waves (parallel to the casting gravity direction) in three different directions (x, y, z), measured parallel ( $V_x$ ) and perpendicularly (two orthogonal directions  $V_y$  and  $V_z$ ) to the casting direction, presence of anisotropy inside the samples can be determined. Namely, if the sample is homogeneous, the minimum dissipation-differences in ultrasonic velocity values in three directions will appear. Contrary, if there are differences of ultrasonic velocities in various directions, it will be an indicator of structural inhomogeneity. The goal of study was to examine whether the material inhomogeneity or anisotropy can cause the accelerated material degradation during the exposure to extreme conditions or thermal shock. This approach was applied to all samples subjected to the testing. Results of ultrasonic velocity values, as a comparative view of the reference samples (cure and dry) as well as the samples sintered at 1100, 1300, and 1600 °C, are shown in Fig. 2 (b). As it is expected, the ultrasonic velocities in all three directions increase with the temperatures of materials treatment induced by reducing porosity and levels of defects inside the samples. Based on the results, it can be concluded that the material structures before the testing are obviously inhomogeneous. Samples sintered at higher temperature showed more pronounced structural homogeneity since the dissipation of ultrasonic velocity ( $\Delta V$ ) was decreased. Hence, the samples sintered at 1600 °C showed almost negligible dissipation of ultrasonic velocities and therefore the highest structural homogeneity. Besides, it was noticed that the values of  $V_y$  and  $V_z$  (perpendicular to the casting directions) are very close mutually while the values of  $V_x$  (parallel to the casting direction) are lower than former two.

It can be concluded that the difference between maximal and minimal values of surface degradation, measure of surface anisotropy, increases in case of samples treated at higher temperature showing increase of the surface anisotropy. Contrary,  $V_{\max}-V_{\min}$ , measure of structural anisotropy, decreases for the samples treated at higher temperatures indicating decrease of the internal anisotropy. Only, the samples sintered at 1300 °C show slightly higher anisotropy and depart from the curve trend. Finally, the samples treated at higher temperature show higher surface anisotropy and lower structural anisotropy.

### 3.2. Longitudinal ultrasonic measurements

In addition to the above analysis, another approach can be realized, too [14]. Fig. 3 shows the velocity of longitudinal ultrasonic waves, measured parallel ( $V_x$ ) and perpendicularly (two orthogonal directions  $V_y$  and  $V_z$ ) to the casting direction, as a function of apparent density.

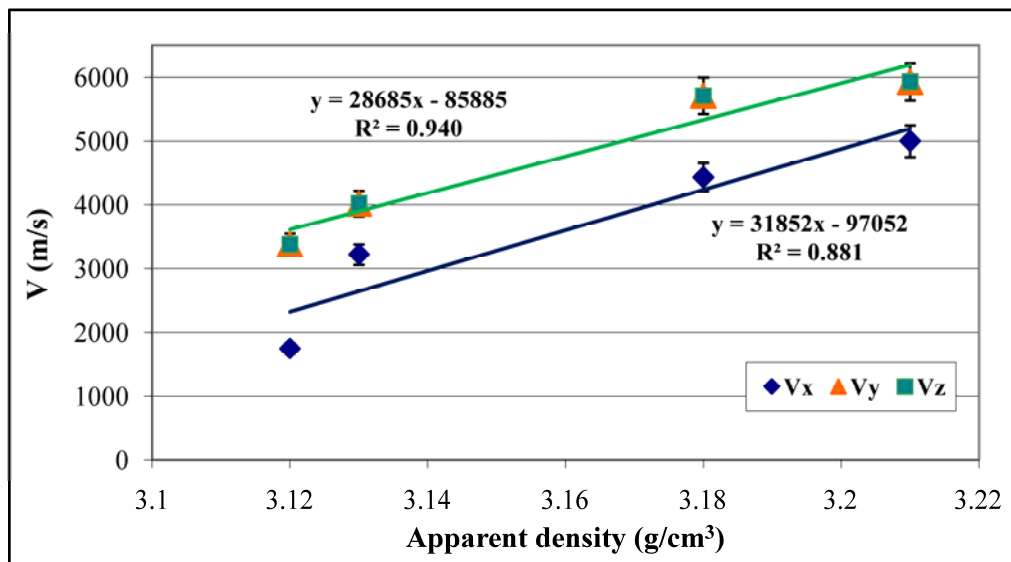


**Fig. 3.** Velocity of longitudinal ultrasonic waves, measured parallel ( $V_x$ ) and perpendicularly (two orthogonal directions  $V_y$  and  $V_z$ ) to the casting gravity direction depending on apparent density.

By the analysis of applied approach, some information can be provided. Namely, it is evident that ultrasonic sound velocities are linearly dependent on apparent densities, so the data clearly fit with linear curves. Further, two orthogonal directions of ultrasonic velocities ( $V_y$  and  $V_z$ ) that are perpendicular to the casting direction are remarkably higher indicating the anisotropy of elastic property. Also, it is obvious that the linear curves ( $V_x$  in comparing with  $V_y$  and  $V_z$ ) are not parallel that is an indicator of changing the elastic anisotropy with density. Based on the information that there is no difference between  $V_y$  and  $V_z$ , the longitudinal wave velocities measured in the two orthogonal directions perpendicular to the casting direction, it can be concluded that the samples are transversely isotropic, e.g. orthotropic. Besides, at last but not least, it is clearly observed that the difference of ultrasonic velocities in parallel ( $V_x$ ) and perpendicular directions ( $V_y$  and  $V_z$ ) to the casting direction are getting decrease with increasing of samples sintering temperature that indicates the decrease of the material anisotropy [14].

Further study has intention to make the analysis of whether the surface or structural anisotropy has the prevailing effects on materials resistance to the thermal shock and how it will change during the testing.

### 3.3 Anisotropy analysis of the samples subjected to the testing

Conventional testing of thermal shock resistance is based on the cyclic heating and cooling of refractory material till the samples surface degrade 50 % of the original surface. It can be assumed that the materials' anisotropy would influence on its behavior during the thermal shock testing. Higher anisotropy before the testing might induce the formation of additional stresses that can cause microcracks formation and growth of already existing ones, and therefore lesser thermal stability.

Based on the results of image analysis and above assumptions and facts, the reference samples and those sintered at 1100 °C before the thermal shock show the lowest surface anisotropy, while the surface anisotropy increases for the samples sintered at higher temperatures. Changes of surface anisotropy during the thermal shock, after each 10 cycles, are calculated as the difference between the highest and the lowest values of surface degradation and the results are presented in Fig. 4.

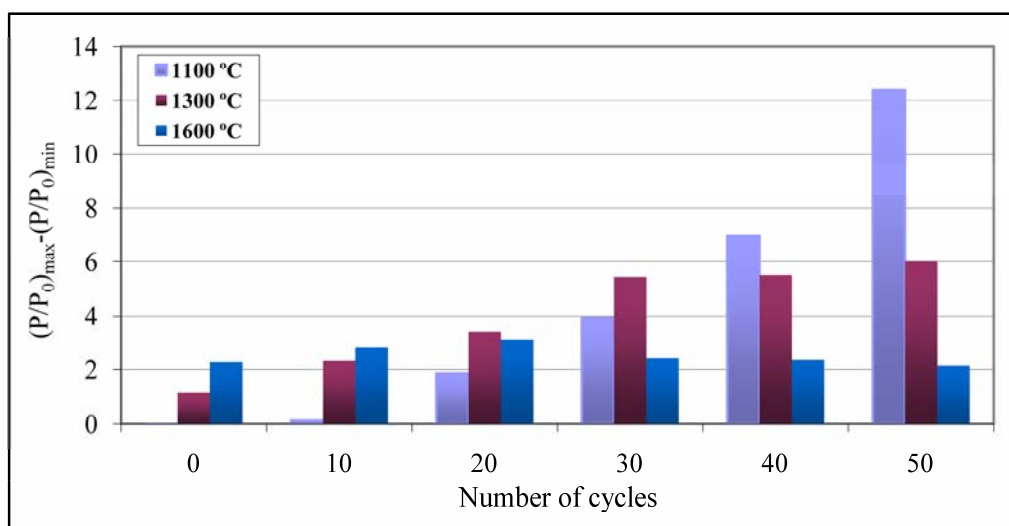


Fig. 4. Surface anisotropy during the thermal shock.

It is obvious that the difference between the highest and the lowest values of surface degradation was growing during the thermal shock in all tested samples [30] and therefore the indicator of surface anisotropy (dissipation of surface degradation level) increases as well. However, with rising of materials' sintering temperature, the dissipation gets smaller and smaller so that the samples sintered at 1600 °C show the dissipation decrease during the thermal shock, i.e. the reduction of surface anisotropy. Although the samples sintered at 1100 °C have the smallest surface anisotropy before the testing, it mostly rises during the thermal shock. Besides, earlier studies [10,12,26,29,30] showed that the degradation of surface in the case of samples sintered at 1100 °C is dominant, so the spalling of the surface during the thermal shock is expected. Precisely, occurrence of the surface spalling can be explained by the highest changes of surface anisotropy. Samples sintered at 1300 °C show slightly higher values of inhomogeneity and anisotropy before the testing, but their anisotropy is changed to a lesser extent during the testing. Namely, samples sintered at 1300 °C behave more stable probably due to smaller dissipation of surface degradation levels during the thermal shock. On the other hand, the samples sintered at 1600 °C showed the highest surface anisotropy before the testing but during the testing surface anisotropy changes were very small and did not exceed 4 % after 40 thermal shock cycles. Earlier study showed that these samples had the tendency toward explosive breakage and the largest compressive strength decrease, so it can

be concluded that the surface anisotropy has no prevail influence on behavior of those samples but structural i.e. internal consistency or homogeneity.

As it is mentioned above, monitoring the structural anisotropy was based on ultrasonic measurements of longitudinal waves (parallel to the casting gravity direction) in three different directions (x, y, z), measured parallelly ( $V_x$ ) and perpendicularly (two orthogonal directions  $V_y$  and  $V_z$ ) to the casting direction. Results of measuring the ultrasonic velocities during the testing are shown in Fig. 5.

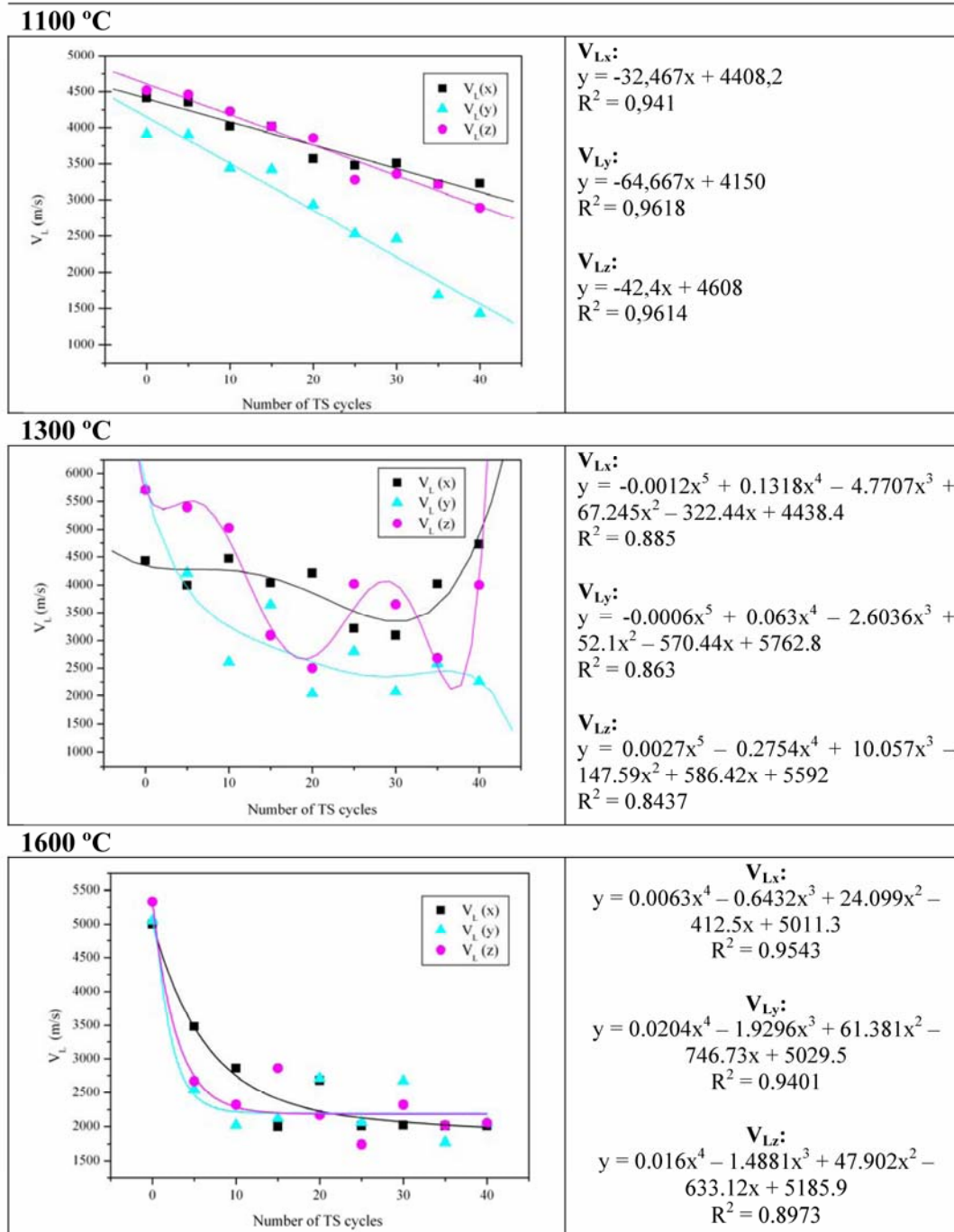


Fig. 5. Ultrasonic velocity of longitudinal waves in three directions during thermal shock.

It is obvious that in case of all samples, ultrasonic velocities have declining trend during the thermal shock showing linear and polynomial dependences with the number of thermal shock cycles.

Samples sintered at 1100 °C show linear dependence with excellent correlation with number of thermal shock cycles  $R^2 > 0.9$ . On the other side, samples sintered at 1300 and 1600 °C fit polynomial regression of the 5<sup>th</sup> and 4<sup>th</sup> degrees, respectively. Samples sintered at 1300 and 1600 °C show coefficient of determination  $R^2 > 0.8$  that indicate strong correlation of fitted curve with the measuring results.

Homogeneity of sample is reflected in minimum dissipation-differences of ultrasonic velocity values in three directions ( $\Delta V = V_{\max} - V_{\min}$ ). Real access and overview between the highest and the lowest values of ultrasonic velocities during the thermal shock is shown in Fig. 6.

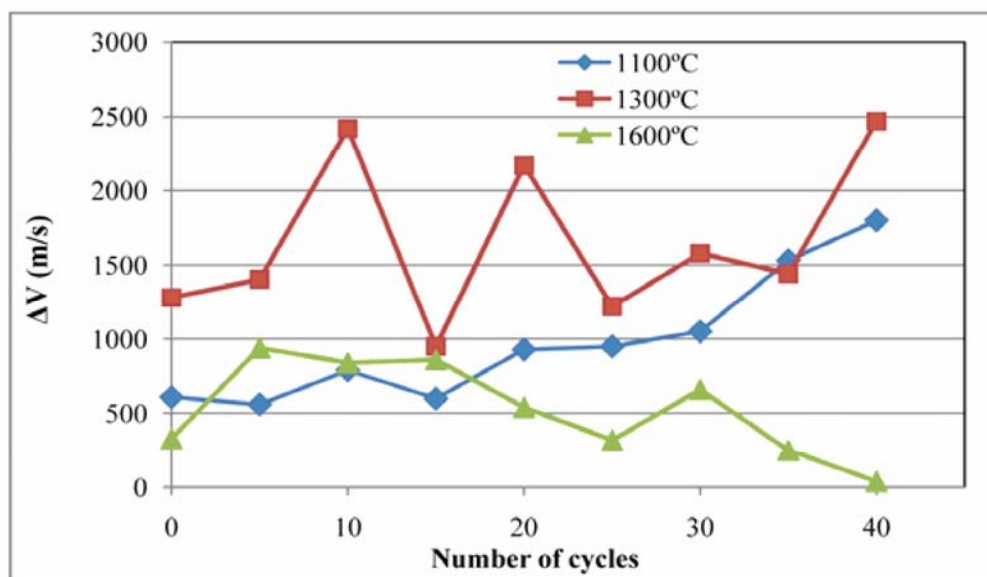
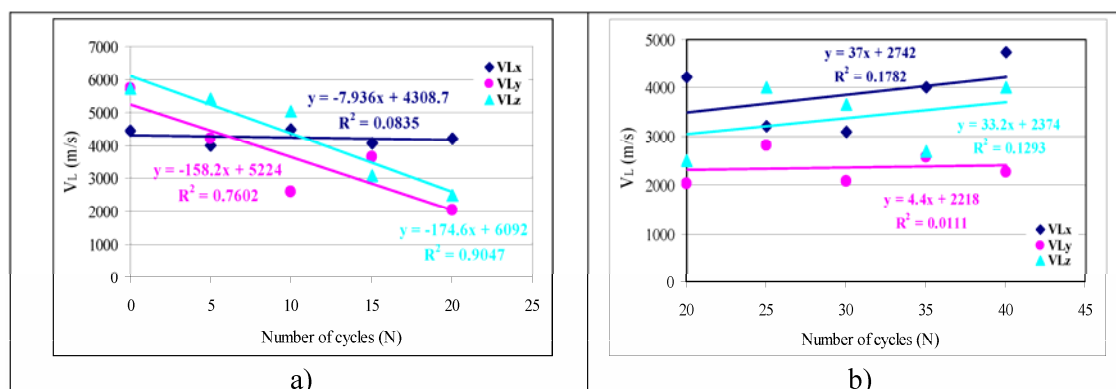


Fig. 6. Levels of ultrasonic velocity dissipation.

Cyclic changes of internal homogeneity are noticed in all tested samples, while the largest variations and the highest anisotropy can be observed in the samples sintered at 1300 °C. Namely, even before thermal shock the samples sintered at 1300 °C have the maximum inhomogeneity and during the testing homogeneity changed cyclically. On the other side, the samples sintered at 1100 and 1600 °C showed lower inhomogeneity of the structure with lesser dissipations. During the testing, anisotropy of the samples sintered at 1600 °C slightly decreases, while the samples sintered at 1100 °C show increase of structural anisotropy. Namely, the highest compressive strength of the samples sintered at 1600 °C before thermal shock [30] can be explained by the smallest internal anisotropy of these samples. Anyway, all changes in homogeneity can be considered as a consequence of the structure rearrangement due to sudden and cyclic changes in temperature. In case of samples sintered at 1100 °C, dependence is linear with high coefficient of correlations with number of thermal shock cycles. During the testing, values of ultrasonic velocities are the lowest in y direction, while the changes in x and z directions are similar having very close values. Dissipations of the ultrasonic velocities in different directions were increasing during the thermal shock. The highest dissipation of ultrasonic velocities in three directions and therefore the largest material inhomogeneity and anisotropy inside the material before and during the thermal shock was observed in the samples sintered at 1300 °C. However, these samples exhibited the greatest stability during the thermal shock, since they withstood 110 cycles of thermal shock without hazardous cracks [10,12,26,27,29,30]. Samples sintered at

1300 °C exhibited polynomial dependences of fifth order during the thermal shock. The negligible dissipations of the ultrasonic velocity values per measured directions were evident for the samples sintered at 1600 °C and therefore material can be considered as a homogeneous and isotropic. However, the decrease of ultrasonic velocities in all directions for the samples sintered at 1600 °C subjected to the thermal shock was the highest and noticeable immediately after 5 cycles of thermal shock. All three directions of ultrasonic velocities are changed according to polynomial decay of fourth order and correlation ( $R^2$ ) with number of thermal shock cycles of around 0.9.

Since the samples sintered at 1300 °C showed the highest dissipations of ultrasonic velocities in measured directions and the highest anisotropy, while on the other side they withstood over 110 cycles of thermal shock and generally were the most stable during the testing [10,12,30], they were subjected to the detailed analysis. Period of monitoring the results of the samples with considerable dissipations were divided into two intervals. The first interval starts from the beginning to 20 cycles of thermal shock and the second one includes the period from 20 to 40 cycles of thermal shock. Graphical comparative approach of gradient changes of ultrasonic velocities per measuring directions during the thermal shock is shown in Fig. 7.



**Fig. 7.** Two intervals of  $V_L$  changes per directions for the samples sintered at 1300 °C: (a) 0-20 and (b) 20-40.

Namely, two different behaviors are noticed on diagrams in regard of measuring directions.

Likewise as in the samples before thermal shock, similar changes in ultrasonic velocities can be observed in y and z directions (perpendicular to the casting direction), while in x direction (parallel to the casting direction) change of ultrasonic velocity during the testing is quite different. Changes of longitudinal ultrasonic velocity waves measured parallel to the casting direction ( $V_x$ ) are negligible during the whole period. This is confirmed by small values of curve slopes for both observed periods. In the first period, relatively large gradients are noticed regarding rate of measured values change ( $V_y$  and  $V_z$ ). After 20 cycles of thermal shock, changes in behavior of materials occurred. Namely, changes in curve slope are evident so that the ultrasonic velocities increase after 20<sup>th</sup> cycle contrary to the testing of the first 20 cycles where the ultrasonic velocities decrease during the testing. This can be considered as the moment of qualitative changes appearance as well as morphology and structure changes. Differences in the gradient of the ultrasonic velocities between the considered intervals indicate that the ``breaking point`` in behavior of the samples sintered at 1300 °C in response to extreme conditions occurred after 20 cycles of thermal shock. Considering the results of regression analysis and their comparison by directions, it can be concluded that in case of all tested samples, the highest correlation coefficient ( $R^2$ ) is in y-direction, which means that changes of ultrasonic velocity of longitudinal wave in y-direction have the best correlation

with the number of thermal shock cycles. Correlation coefficients in all directions are around 0.9 considering as strong correlation with the number of thermal shock cycles.

#### 4. Conclusion

Overall review of the results implies that the surface anisotropy has prevailing influence on behavior of material during the thermal shock in regard to the structural one. According to applied approach, dissipation-differences among the levels of degradation per surface sides were used as an indicator of surface anisotropy while the structural anisotropy was monitored by dissipation differences between the values of ultrasonic velocities among three different directions. All tested samples are inhomogeneous before the testing, but samples sintered at higher temperature showed more pronounced structural homogeneity; samples sintered at 1600 °C showed the highest structural homogeneity while the samples sintered at 1300 °C exhibited slightly higher anisotropy and small digression from the curve trend. Ultrasonic velocities are linearly dependent on apparent densities. Two orthogonal directions of ultrasonic velocities are remarkably higher indicating the anisotropy of elastic property. Since the linear curves ( $V_x$ ,  $V_y$ , and  $V_z$ ) are not parallel, there is a change of elastic anisotropy with density. There is no difference between  $V_y$  and  $V_z$ , so the samples are transversely isotropic, e.g. orthotropic. The difference of ultrasonic velocities in parallel ( $V_x$ ) and perpendicular directions ( $V_y$  and  $V_z$ ) to the casting direction is decreasing with increasing of samples' sintering temperature indicating the decrease of the material anisotropy. Generally, the samples treated at higher temperature show higher surface anisotropy and lower structural anisotropy.

During the testing of thermal shock, cyclic changes of internal homogeneity are noticed in all tested samples. The anisotropy of the surface was decreased in the samples sintered at higher temperature. The samples sintered at 1100 and 1600 °C showed lower inhomogeneity of the structure with lesser dissipations during the testing. Even, the anisotropy character of the samples (surface and structural) sintered at 1600 °C slightly decreased during the thermal shock. The largest dissipations of the ultrasonic velocities and the highest structural anisotropy during the testing were observed in the samples sintered at 1300 °C. However, these samples have been proved as the most stable during the testing, so that they were subjected to the detailed analysis. "Breaking point" in behavior of the material is noticed at 20<sup>th</sup> cycle so the whole period of monitoring can be divided into two intervals. There are no changes in  $V_x$  direction while  $V_y$  and  $V_z$  remarkably decreased indicating the increase of porosity level. Also, dissipations of data points are minimum up to 20<sup>th</sup> cycle of thermal shock, however after 20 cycles dissipations of data points are significant, while the curves exhibit an opposite trend.

#### Acknowledgments

This research has been financed by the Ministry of Education, Science and Technological Development of Republic of Serbia as a part of the project TR 33007. The authors would like to express their gratitude for this support.

#### 5. References

1. D. Boccaccini, M. Romagnoli, P. Veronesi, M. Cannio, C. Leonelli, G. Pellacani, T. Volkov-Husovic, A. Boccaccini, *Int. J. Appl. Ceram. Tec.*, 4(3) (2007) 260-268.

2. S. Marenovic, M. Dimitrijevic, T. Volkov-Husovic, B. Matovic, *Ceram. Int.*, 35(3) (2009) 1077-1081.
3. E.A. Dean, J.A. Lopez, *J. Am. Ceram. Soc.*, 66(5) (1983) 366-370.
4. F. Cardoso, M. Innocentini, M. Miranda, F. Valenzuela, V. Pandolfelli, *J. Eur. Ceram. Soc.*, 24 (2004) 797-802.
5. C. Parr, B. Valdelicvre, C. Wöhremeyer, *Refract. Appl. News*, 7(3) (2002) 17-23.
6. M.D.M. Innocentini, A.R.F. Pardo, V.C. Pandolfelli, B.A. Menegazzo, L.R.M. Bittencourt, R.P. Rettore, *J. Am. Ceram. Soc.*, 85(6) (2002) 1517-1521.
7. F.A. Cardoso, M.D.M Innocentini, M.M. Akiyoshi, V.C. Pandolfelli, *Refract. Appl. News*, 9(2) (2004) 12-16.
8. S. Maitra, S. Bose, N. Bandyopadhyay, *Ceram. Int.*, 31 (2005) 371-374.
9. A.R. Studart, R.G. Pileggi, V.C. Pandolfelli, J. Gallo, 80(11) (2001) 34-39.
10. S. Martinovic, M. Vlahovic, T. Boljanac, M. Dojcinovic, T. Volkov-Husovic, *J. Eur. Ceram. Soc.* 33 (2013) 7-14.
11. J.M. Auvray, C. Gault, M. Huger, *J. Eur. Ceram. Soc.*, 27 (2007) 3489-3496.
12. S. Martinovic, M. Dojcinovic, M. Dimitrijevic, A. Devecerski, B. Matovic, T. Volkov-Husovic, *J. Eur. Ceram. Soc.*, 30 (2010) 3303-3309.
13. C. Leonlli, F. Bondioli, P. Veronesi, M. Romagnoli, T. Manfredini, G. Pellacani, V. Cannillo, *J. Eur. Ceram. Soc.*, 21 (2001) 786-793.
14. M. Romagnoli, M. Lassinantti Gualtieri, A.F. Gualtieri, R. Šliteris, R. Kažys, G. Tari, *J. Eur. Ceram. Soc.*, 33 (2013) 2785-2792.
15. D.S. Kupperman, H.B. Karplus, *Am. Ceram. Soc. Bull.*, 63 (1984) 1505-1509.
16. M.P. Jones, G.V. Blessing, C.R. Robbins, *Mater. Eval.*, 44 (1986) 859-862.
17. R.A. Roberts, *Mater. Eval.*, 46 (1988) 758-766.
18. C.H. Schilling, V.J. Garcia, R.M. Smith, *J. Am. Ceram. Soc.*, 81 (1998) 2629-2639.
19. M.C. Bhardwaj, *Ceram. Trans.*, 89 (1998) 265-281.
20. T.J. Carneim, D.J. Green, M.C. Bhardwaj, *Am. Ceram. Soc. Bull.*, 78 (1999) 88-94.
21. S.D. Aston, R.E. Challis, G.P. Yiasemides, *Nondest. Test. Eval.*, 17 (2001) 263-273.
22. G.M. Revel, *Exp. Mech.*, 47 (2007) 637-648.
23. M. Romagnoli, M. Burani, G. Tari, J.M.F. Ferreira, *J. Eur. Ceram. Soc.*, 27 (2007) 1631-1636.
24. A. Shui, Z. Kato, T. Satashi, N. Uchida, K. Uematsu, *J. Eur. Ceram. Soc.*, 22 (2002) 311-316.
25. Image Pro Plus, Version 4.0 for Windows, Media Cybernetics, Silver Spring.
26. T. Volkov Husovic, *J. Test. Eval.*, 35(1) (2006) 1-5.
27. T. Volkov Husovic, S. Martinovic, M. Dimitrijevic, M. Dojcinovic, J. Majstorovic, B. Matovic, Nondestructive evaluation methods for composites: ultrasonic measurements and image analysis application on testing in extreme conditions, in: L. Nicolais, A. Borzacchiello (Eds.), *Encyclopedia of composites*, Hoboken, New Jersey: Publisher John Wiley & Sons, 2012, pp. 1-6.
28. M. Vlahovic, P. Jovanic, S. Martinovic, T. Boljanac, T. Volkov Husovic, *Compos. Part B*, 44 (2013) 458-466.
29. S. Martinovic, J. Majstorovic, V. Vidojkovic, T. Volkov-Husovic, *Ceram.–Silikaty*, 54(2) (2010) 169-175.
30. S. Martinovic, M. Vlahovic, T. Boljanac, J. Majstorovic, T. Volkov Husovic, *Compos. Part B*, 60 (2014) 400-412.
31. D.N. Boccaccini, C. Leonelli, M.R. Rivasi, M. Romagnoli, A.R. Boccaccini, *Ceram. Int.*, 31(3) (2005) 417-432.
32. D. Kumar Pandey, S. Pandey, *Ultrasonics: A Technique of Material Characterization*, in: D.W. Dissanayake (Ed.), *Acoustic Waves*, Sciyo, Croatia; 2010, pp. 397-431.

- 
- 33.W.P. Mason, Physical acoustics and properties of solids, D. Van Nostrand Co., Princeton, New York, vol. 13, 1958, pp. 368-373.
- 34.R.L. Singhal, Solid State Physics, Keda Nath Ram Nath&Co. Publishers, Meerut, India, 2003.

---

**Садржај:** *Анализиран је високо-алуминатни нискоцементни ватростални бетон синтерован на три различите температуре. Испитиван је утицај почетне анизотропије материјала на отпорност на термошок, као и промене нивоа анизотропије током термошока. Као експериментални метод за испитивање термостабилности коришћен је тест каљењем у води. Анализа слике је коришћена за анализу површинске анизотропије, док је структурна анизотропија праћена ултразвучним мерењима. Резултати су показали да узорци синтеровани на 1600 °C имају највећу хомогеност и најмању структурну и површинску анизотропију. Површинска анизотропија има већи утицај на понашање материјала током термошока, док структурну анизотропију не треба занемарити.*

**Кључне речи:** *Ватростални материјали, анизотропија, анализа слике, ултразвучна мерења, нискоцементни бетон*

---